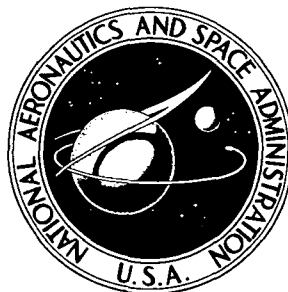


**NASA TECHNICAL  
MEMORANDUM**



**NASA TM X-3055**

**NASA TM X-3055**

**CASE FILE  
COPY**

**BURNING OF SOLIDS  
IN OXYGEN-RICH ENVIRONMENTS  
IN NORMAL AND REDUCED GRAVITY**

*by Charles R. Andracchio and Thomas H. Cochran*

*Lewis Research Center*

*Cleveland, Ohio 44135*



1. Report No. <b>NASA TM X-3055</b>	2. Government Accession No.	3. Recipient's Catalog No.	
4. Title and Subtitle <b>BURNING OF SOLIDS IN OXYGEN-RICH ENVIRONMENTS IN NORMAL AND REDUCED GRAVITY</b>		5. Report Date <b>MAY 1974</b>	6. Performing Organization Code
		8. Performing Organization Report No. <b>E-7848</b>	
7. Author(s) <b>Charles R. Andracchio and Thomas H. Cochran</b>		10. Work Unit No. <b>502-24</b>	11. Contract or Grant No.
9. Performing Organization Name and Address <b>Lewis Research Center National Aeronautics and Space Administration Cleveland, Ohio 44135</b>		13. Type of Report and Period Covered <b>Technical Memorandum</b>	
		14. Sponsoring Agency Code	
12. Sponsoring Agency Name and Address <b>National Aeronautics and Space Administration Washington, D.C. 20546</b>		15. Supplementary Notes	
16. Abstract <p>An experimental program was conducted to investigate the combustion characteristics of solids burning in a weightless environment. The combustion characteristics of thin cellulose acetate material were obtained from specimens burned in supercritical as well as in low pressure oxygen atmospheres. Flame spread rates were measured and found to depend on material thickness and pressure in both normal gravity (1-g) and reduced gravity (0-g). A gravity effect on the burning process was also observed; the ratio of 1-g to 0-g flame spread rate becomes larger with increasing material thickness. Qualitative results on the combustion characteristics of metal screens (stainless steel, inconel, copper, and aluminum) burning in supercritical oxygen and normal gravity are also presented. Stainless steel (300 sq mesh) was successfully ignited in reduced gravity; no apparent difference in the flame spread pattern was observed between 1-g and 0-g.</p>			
17. Key Words (Suggested by Author(s)) <b>Combustion      Supercritical oxygen Flame spread    Space cabin atmospheres Zero gravity</b>		18. Distribution Statement <b>Unclassified - unlimited Category 33</b>	
19. Security Classif. (of this report) <b>Unclassified</b>	20. Security Classif. (of this page) <b>Unclassified</b>	21. No. of Pages <b>20</b>	22. Price* <b>\$3.00</b>

# BURNING OF SOLIDS IN OXYGEN-RICH ENVIRONMENTS IN NORMAL AND REDUCED GRAVITY

by Charles R. Andracchio and Thomas H. Cochran

Lewis Research Center

## SUMMARY

An experimental program was conducted to investigate the combustion characteristics of solids burning in a weightless, pure oxygen environment. Flame spread rates were measured on cellulose acetate specimens that were 0.0025, 0.0051, and 0.0122 centimeter (0.001, 0.002, 0.0048 in.) thick. The samples were burned in a supercritical oxygen atmosphere at 634 newtons per square centimeter,  $-118^{\circ}$  C (920 psia,  $-180^{\circ}$  F) as well as in low pressure atmospheres at 3.45 and 10.14 newtons per square centimeter,  $20^{\circ}$  C (5 and 14.7 psia,  $68^{\circ}$  F).

Flame spread rates were found to depend on material thickness in both normal gravity (1-g) and reduced gravity (0-g); an increase in thickness results in a lower flame spread rate. The ratio of 1-g to 0-g flame spread rate increased with increasing thickness. Likewise, an effect of pressure was observed; an increase in pressure produces an increase in spread rate. Qualitative results on the combustion characteristics of metal screens (stainless steel, inconel, copper, aluminum, and titanium) burning in supercritical oxygen in normal gravity are also presented. A stainless steel screen (300 sq mesh) was successfully ignited in reduced gravity; no apparent difference in flame spread pattern was observed between 1-g and 0-g.

## INTRODUCTION

A fire occurring in an oxygen-rich environment propagates relatively fast and usually leads to destructive and sometimes fatal results (ref. 1). The necessary use of these environments in such applications as the U.S. space program, hospitals, compression chambers, and other various industrial uses emphasizes the importance of investigating new measures to reduce this fire hazard.

One aspect of the problem concerns the combustion of solid materials. Once the

mechanism of flame spread over the surface of a solid is understood, improved fire safety techniques can be developed. Several references on solid combustion have appeared in the literature during the last few years. Theoretical models have been proposed (refs. 2 to 6) in which flame spread rate is dependent on environmental gas phase properties as well as properties of the solid fuel. Huggett (ref. 6) reported that the flame spread rate was inversely proportional to the fuel thickness for a thin vertical sheet burning downward. In addition, he also correlated flame spread rate with the specific heat of the atmospheric mixture per mol of oxygen present. In references 2 and 3 a further delineation of the thickness dependency was made; thermally thin and thermally thick solid fuels were defined. Other reported information on flame spread rate are given in references 7 to 10.

The previous references neglect the effect of gravity on the burning process. Tests conducted at the Lewis Research Center (ref. 11) indicate that burning can occur under reduced-gravity conditions. In the case of solids, the burning was accompanied by a well-defined flame which propagated over the surface at a lower rate than in normal gravity. No signs of extinguishment were observed until the flame completely enveloped the surface. Other reported literature on gravity effects are given in references 12 to 19. Kimzey (ref. 12) reported that steady-state conditions during the burning of a solid in zero-g does not exist once surface combustion has taken place.

At the present time, experimental data available on flame spread rates in reduced gravity levels are scarce. The purpose of this report, then, is to present the results of a study on the burning characteristics of several solid fuels in one-g and zero-g environments. Data are presented regarding flame spread over cellulose acetate specimens burning in a reduced-gravity environment in a 100 percent oxygen atmosphere; in addition, qualitative data obtained for burning metals are also presented. Results were obtained for low pressure atmospheres ( $3.45 \text{ N/cm}^2$  (5 psia) and  $10.14 \text{ N/cm}^2$  (14 psia)) as well as for a supercritical oxygen atmosphere ( $634 \text{ N/cm}^2$ , 920 psia). A comparison between the normal and reduced gravity data is made, and similarities with the present normal gravity theories are discussed.

## SYMBOLS

C	specific heat of gaseous phase
$C_s$	specific heat of solid fuel bed
$F(P, Y_{\text{OX}})$	dimensionless integral used in ref. 4 for representing an implicit function of pressure and oxygen mol fraction
K	thermal conductivity of gaseous phase

P	combustion chamber pressure
$Q_c$	heat released per unit of solid fuel burned
$T_B$	vaporization temperature of solid fuel bed
$T_0$	initial temperature of solid fuel bed
V	flame spread velocity
$Y_{ox}$	oxygen mol fraction of gaseous phase
$\rho_s$	density of solid fuel bed
$\tau$	thickness of solid fuel bed

## APPARATUS AND PROCEDURE

### Supercritical Oxygen Tests

Test facility. - All tests conducted in supercritical oxygen were performed at Lewis Research Center in the 5-second Zero Gravity Facility. The principal method of obtaining reduced gravity in the facility is to allow the experiment to free fall in a vacuum through a distance of 122.5 meters. There were no external connections or guide wires attached to the free falling experiment, and thus no external forces (aside from gravity) were present except residual air drag. The effective maximum gravitational acceleration acting on the experiment was estimated to be of the order of  $10^{-5}$  g. For a complete description of the Zero Gravity Facility the reader should refer to the appendix in reference 15.

Experimental apparatus. - The experimental combustion apparatus is shown in schematic form in figure 1. The essential components include a high speed camera, a combustion chamber, a fuel specimen holder, and an igniter. A 16-millimeter high-speed camera operated at a nominal speed of 400 frames per second and used a 25 millimeter lens. The camera was loaded with Ektachrome EF type 7242 color film. The cylindrically shaped combustion chamber was made of stainless steel and had an internal volume of 1245.6 cubic centimeters. The front end of the chamber contained a 2.54-centimeter-diameter window through which the burning samples were photographed. An expansion tank attached to the back end of the combustion chamber and separated by a burst disk was used as a safety precaution in case of excessive pressure rise. Liquid nitrogen cooling coils were used as an aid in filling the chamber with high pressure, low temperature oxygen. The initial test conditions of the oxygen in the closed chamber were 634 newtons per square centimeter at  $-118^{\circ}$  C ( $920$  psia at  $-180^{\circ}$  F). A thermocouple and pressure transducer were used to record the conditions inside the chamber.

The fuel specimen was clamped between two circular ceramic rings which were pressed together by two sections of stainless steel. This assembly gave a circular burning area of 30.20 square centimeters. The tests were conducted with the samples vertically oriented with respect to the gravity vector as shown in the schematic in figure 1. The igniter, a 26 gage nichrome wire approximately 2.54 centimeters long, was mounted behind the specimen. Ignition was obtained by applying 10 amperes through the igniter for a 1.0 second interval. The holder and igniter were fastened to a metal insert which then fit into the combustion chamber. Figure 2 shows the specimen holder and igniter attached to the metal insert.

Test materials. - Two types of material specimens were tested in this environment, plastics and metals. The plastics were cellulose acetate samples that were 0.0025, 0.0051, and 0.0122 centimeter thick. These materials were clear transparent sheets with a high gloss finish (further specified by MIL-SPEC LP-504). The various metal screens burned included stainless steel (300 sq mesh), inconel (200 sq mesh), copper (100 sq mesh), aluminum (50 sq mesh), and titanium (16 sq mesh).

Test procedure. - Before each test the combustion chamber was thoroughly cleaned using a degreasing solvent and the test specimen was assembled and then installed in the chamber. The chamber was sealed, purged with gaseous oxygen, and then pressurized to the desired test conditions. The latter was accomplished by filling the chamber with gaseous oxygen at a set pressure while cooling the experiment to  $-130^{\circ}\text{C}$  by flowing liquid nitrogen through the cooling coils. The combustion chamber was then allowed to heat to the desired test temperature ( $-118^{\circ}\text{C}$ ). At this point the pressure was checked and, if it was too high, it was decreased to the desired value by venting. The chamber was again cooled to approximately  $-180^{\circ}\text{C}$  and the experiment package mounted in the vacuum chamber of the Zero Gravity Facility. The vacuum chamber was then pumped down and the temperature and pressure in the combustion chamber were monitored. When the required test conditions were reached, the package was released to begin the zero gravity free fall.

### Low Pressure Oxygen Tests

Test facility. - The low pressure data presented in this report were obtained at Lewis Research Center in the 2.2-second Drop Tower. The free fall method of obtaining low gravity environments is also used in this facility, but the air drag is reduced by using a drag shield. The maximum effective acceleration acting on the experiment is of the order of  $10^{-5}$  g. A detailed description of this facility is given in reference 11.

Experimental apparatus. - The experimental combustion apparatus schematically shown in figure 3 consisted of a combustion chamber, a high speed camera, a fuel specimen holder, and an igniter. The combustion chamber (30.5 cm diam, 61 cm high) was

made of stainless steel and had an internal volume of approximately  $445 \times 10^2$  cubic centimeters. Four pyrex glass ports equidistant around the chamber were available for installing and viewing the material under test. The test specimen was held in place by a specimen holder mounted to the base of the combustion chamber. A mirror attached to the near flange of the chamber and positioned at a  $45^\circ$  angle to the test specimen provided a top view of the burning material. The materials were oriented in a horizontal direction with respect to the gravity vector as shown in the schematic diagram. The specimen holder is shown in figure 4 in its approximate position relative to the top-view mirror. The test materials were clamped between two pieces of blued-steel shim stock which resulted in a square burning area of 6.3 centimeters on each side. Also shown in the figure is the nichrome ribbon igniter which was operated by two time delay relays and a dc battery.

The 16-millimeter high speed camera was operated at approximately 400 frames per second using Ektachrome EF type 7242 color film. A digital clock accurate to 0.01 second was always in view of the camera lens.

Test materials. - Cellulose acetate specimens identical to those used in the super-critical oxygen tests were used in the low pressure tests. However, as mentioned previously, the materials were square (6.3 by 6.3 cm) and were burned in a horizontal orientation inside the combustion chamber.

Test procedure. - Prior to each test, the combustion chamber was vacuumed and wiped clean of any residue left from the previous run. The material was then clamped in the specimen holder and adjusted to slightly contact the igniter wire and the complete assembly was installed in the chamber. The combustion chamber was subsequently sealed and pumped down by means of an air aspirator to approximately 0.55 newton per square centimeter absolute (0.80 psia). Following this the chamber was cycled twice through a pressurizing and depressurizing process with oxygen (normally 99.6 percent pure) to 10.3 and 0.55 newton per square centimeter absolute (15 and 0.80 psia), respectively, and finally it was brought to its operating pressure, either 3.45 newtons per square centimeter absolute (5 psia) at  $20^\circ$  C or 10.14 newtons per square centimeter (14.7 psia) at  $20^\circ$  C.

## DATA REDUCTION

The burning samples were photographed on high speed film which was then examined on a motion picture analyzer. Flame spread rates were obtained by measuring the displacement of the flame front from the center, or ignition point of the material, as a function of time. Displacement against time curves were drawn, and their slopes were calculated to obtain the average flame spread rates. The estimated error involved in

measuring the displacements was  $\pm 0.05$  centimeter, which resulted in a maximum error in burning rates of 3 percent.

For the horizontally oriented specimens the spread rate was determined from an average of the left and right edge displacement of the flame front. This was done for both the normal and reduced gravity tests. For the vertically oriented specimens only displacements in the downward direction of flame travel were measured in normal gravity; in reduced gravity four directions of travel (upward, downward, left, and right) were measured and averaged to determine the spread rate. The flame spread rates in each direction of travel were essentially the same for a specified material and g-level.

## RESULTS AND DISCUSSION

### General Observations

Cellulose acetate. - Figure 5 shows a typical flame produced by cellulose acetate samples burning in supercritical oxygen. In normal gravity (1-g) the flame appears plume shaped at 0.05 second after ignition and smoke is being generated near the top of the flame. At 0.10 second the plume is better defined and the smoke is observed to circulate about the chamber. In contrast, the flame in reduced gravity (0-g) has no plume, spreads in a circular pattern, and generates less smoke. The flame color was bright yellow, almost white in 1-g, whereas burning in 0-g resulted in an orange colored flame. (The lines that appear in the 0-g photographs are small cracks that occurred on the original film; these cracks were caused by the low vacuum environment of the Zero Gravity Facility.)

Similar results were observed in the low pressure oxygen tests. Figure 6 shows cellulose acetate burning in 3.45 newtons per square centimeter oxygen. The specimen is horizontally oriented. Again no plume appeared in zero-g. The burning specimen produced a flattened, hemispherical-shaped flame symmetrically positioned about the top and bottom surface of the sample. The image in the mirror shows a circular spread pattern. In normal gravity the flame was brighter and became plume shaped on the top surface. On the bottom surface the flame was flat and its leading edges were slightly ahead of the flame on the top surface. The flame was less intense at the low pressure as compared to the supercritical data, and it exhibited small localized spots where bubbling and spurting occurred. This behavior was not observed in the supercritical tests. It seemed as if small pockets of gases were trapped in localized areas within the flame and began exploding. This condition was characteristic of all plastic specimens at low pressures and was more pronounced in zero-g.

Metals. - The metals could not be ignited by simple contact at the igniter with the specimen. A small strip of cellulose acetate wrapped around the nichrome wire finally



resulted in successful ignition of all the metals in 1-g. However, good photography was difficult to obtain; the specimens burned with such intensity as to overexpose much of the test film. The best representative photograph of a metal burning in supercritical oxygen is shown for stainless steel in figure 7. At both gravity levels the flame seemed to be composed of individual liquid or gaseous globules which continued to burn and sometimes burst into smaller particles. The screen geometry may have contributed to this effect. More smoke can be seen generated in 1-g and the particles are more intense; nevertheless, there was no apparent difference in the pattern of the flame spread.

Inconel and copper exhibited partial burning in 1-g. Once ignited, the inconel screen seemed to turn to a liquid mass in the vicinity of the flame; the burning liquid then fell toward the bottom of the screen igniting fresh surfaces in its path and finally was self-extinguished. As a result, only 20 percent of the screen was burned, and the bulk of this burning was in the downward direction. Identical results occurred with copper with roughly 10 percent of its surface burning before self-extinguishment took place. The flame produced by burning aluminum and titanium was too bright to distinguish any spread pattern on the film. Both metals were completely burned when the combustion chamber was dismantled. The titanium sample damaged the ceramic holder during burning. Because of the difficulties involved with ignition, photography, incomplete combustion, and high intensity of the burning metals, copper, aluminum, titanium, and inconel were not tested in 0-g.

### Flame Spread Rates

Cellulose acetate. - Figure 8 shows the dependency of flame spread rate on fuel thickness for both the supercritical and low pressure test conditions. Several general observations can be made from this figure. First, the flame spread rate decreases as thickness increases. The slopes of these curves rise sharply as the material thickness decreases below approximately 0.006 centimeter; this indicates a rapid increase in the flame spread rate. Similar results for 1-g burning were reported by other investigators. Huggett (ref. 6) and Lastrina (ref. 4) both experimentally measured and analytically showed flame spread rate to be inversely proportional to thickness for a thin sheet burning in a downward direction. Data for downward burning vertical specimens obtained for this report are presented in figure 8(c) and they generally support the inverse proportionality viewpoint. Moreover, it appears from figures 8(a) and (b) that the horizontal burning specimens also follow the same trend. Furthermore, the trend is the same in 0-g as in 1-g over the range of thicknesses tested.

A second observation from figure 8 is that the flame propagation rate in 0-g is always less than in 1-g. Overall, the difference is less than one order of magnitude as shown by the spread rate values in table I.

An effect of pressure on flame spread rate was also observed. Examining the 0-g data, the rate for the thinnest sample at 3.45 and 10.14 newtons per square centimeter is 5.5 centimeters per second; increasing the pressure to 634 newtons per square centimeter corresponds to a propagation rate of 9.7 centimeters per second, which is almost a two-fold increase. Similar results were noted for the thickest material where as much as a fourfold increase was observed.

The increase in spread rate with pressure merits further discussion. In reference 4 an analytical model of flame propagation over solid fuels resulted in the following equation for a thermally thin material:

$$V \cong \frac{KQ_c Y_{ox} F(P, Y_{ox})}{\rho_s C_s C \tau (T_B - T_0)}$$

This equation simply relates the flame spread rate  $V$  with properties of the solid fuel and properties of the gaseous environment. For the experimental conditions described in this report  $T_0$ , the initial temperature of the fuel and surrounding environment, had values of 293 K for the low pressure tests and 155 K for the supercritical oxygen tests. Evaluating the gaseous properties at a mean temperature

$$\bar{T} = \frac{T_{\text{flame}} + T_0}{2}$$

results in a change in the ratio of thermal conductivity to specific heat ( $K/C$ ) between both initial conditions of approximately 5 percent. If it is assumed that the solid phase properties density and specific heat ( $\rho_s$  and  $C_s$ ) are relatively insensitive to temperature and that the heat released per unit of fuel burned ( $Q_c$ ), the thickness of the fuel ( $\tau$ ), and the oxygen mol fraction of the environment ( $Y_{ox}$ ) are constant for a given fuel at a specified test condition, the equation can then be expressed as

$$V \propto \frac{F(P, Y_{ox})}{(T_B - T_0)}$$

A log-log plot of  $V(T_B - T_0)$  against  $P$  for the thinnest material tested is shown in figure 9 using the estimated value of  $T_B = 643$  K (evaporation temperature of solid fuel given in ref. 4 for a plastic material). The slope of a linear curve fit through the available data points by a least square method yields 0.15 for normal gravity and 0.18 for zero gravity. These results resemble Lastrina's in reference 4 which indicate a slight pressure effect ( $P^{0.1}$ ) for thin cellulosic materials and also polymethylmethacrylate.

The thicker cellulose acetate materials (0.0051 and 0.0122 cm) in normal gravity exhibited a greater dependency on pressure with the burning rate being proportional to  $P^{0.3}$  and  $P^{0.4}$ , respectively. The reported burning rate dependency on pressure (ref. 4) for thick cellulosic specimens was  $P^{0.63}$  and for polymethylmethacrylate was  $P^{0.82}$ . Thus, both 0.0051- and 0.0122-centimeter-thick cellulose acetate specimens are probably in a transition state between thermally thin and thermally thick regions.

When analyzing the normal gravity data it should be noted that the specimens at the supercritical condition were burned in a vertical orientation while those at low pressure were burned in a horizontal orientation. However, it has been shown in references 6 and 11 that the vertical downward spread rate is the same as the horizontal spread rate in normal gravity.

To compare the 1-g and 0-g data a ratio of normal gravity to zero gravity spread rate is plotted against thickness in figure 10. Any effects of combustion chamber geometry or initial temperature are ordered out because these variables were fixed for a given set of 1-g to 0-g data. For very thin burning samples the value of the ratio approaches unity and as the thickness increases the ratio becomes larger. Apparently the slower propagating flames obtained with thick samples have a greater proportion of their combustion process affected by gravity driven convection. For this particular material tested the ratio seems to approach a value of 2. From another viewpoint, the reduced gravity spread rate approaches one-half the value obtained in normal gravity as the thickness of the fuel increases.

Metals. - As mentioned in the General Observations section, the metals were difficult to ignite, burned very intensely, and overexposed much of the test film. Since the available test data with stainless steel exhibited an irregular flame front, it was not possible to perform representative spread rate measurements.

## SUMMARY OF RESULTS

The following results were observed from the data obtained with the cellulose acetate specimens in both high and low pressure oxygen environments:

1. Flame spread rate depends on the thickness of the material in both normal and zero gravity. An increase in thickness results in a decrease in flame spread rate.
2. The ratio of 1-g to 0-g flame spread rate appears to be unity for very thin materials and becomes larger with increasing material thickness.
3. Flame spread rate depends on pressure; an increase in pressure increases flame spread rate. For the thinnest specimen tested, flame spread rate exhibited a minor dependency on pressure (of the order of  $P^{0.1}$ ). The effect of pressure in 0-g is approximately the same as 1-g.

The following are observations on the metal specimens:

1. Stainless steel, inconel, copper, and aluminum were successfully ignited in supercritical oxygen, normal gravity.

2. Stainless steel screen was successfully ignited in 0-g. The intensity of the flame was greater in 1-g, but there appeared to be no difference in spread pattern. The specimen burst into separate globules which continued to burn under both gravity levels.

Lewis Research Center,  
National Aeronautics and Space Administration,  
Cleveland, Ohio, February 27, 1974,  
502-24.

#### REFERENCES

1. Ordin, Paul M.: Mishaps with Oxygen in NASA Operations. NASA TM X-67953, 1971.
2. DeRis, N. J.: Spread of a Laminar Diffusion Flame. Twelfth Symposium (International) on Combustion, The Combustion Institute, 1969, pp. 241-252.
3. Lastrina, Frank A.: Flame Spreading Over Solid Fuel Beds: Solid and Gas Phase Energy Considerations. Ph.D. Thesis, Stevens Inst. of Tech., 1970.
4. Magee, Richard S.; and McAlevy, Robert F.: The Investigation of Flame Spreading over the Surface of Igniting Solid Propellants, Final Summary Report. ME-RT-70009, Dept. of Mechanical Eng., Stevens Inst. of Tech. (NASA CR-111942), 1971.
5. Tarifa, Carlos S.; Notario, Pedro P.; Torralbo, Antonio M.: On the Process of Flame Spreading over the Surface of Plastic Fuels in an Oxidizing Atmosphere. Twelfth Symposium (International) on Combustion, The Combustion Institute, 1969, pp. 229-240.
6. Huggett, Clayton; von Elbe, Guenther; and Haggerty, Wilburt: The Combustibility of Materials in Oxygen-Helium and Oxygen-Nitrogen Atmospheres. SAM TR-66-85, Atlantic Research Corp. (AD-489728), 1966.
7. Kuchta, J. M.; Furno, A. L.; Martindill, G. H.; Litchfield, E. L.; and Kubala, T. A.: Flammability of Fabrics and Other Materials in Oxygen-Enriched Atmospheres. Fire Tech., vol. 5, no. 3, Aug. 1969, pp. 203-216.
8. Sirignano, W. A.: A Critical Discussion of Theories of Flame Spread Across Solid and Liquid Fuels. Combustion Sci. and Tech., vol. 6, nos. 1-2, Sept. 1972, pp. 95-105.

9. Nakakuki, Atsumi: Flame Spread Rates of Solid Combustibles in Compressed and Oxygen-Enriched Atmospheres. Jour. Fire and Flammability, vol. 3, Apr. 1972, pp. 146-152.
10. Campbell, Ashley S.: Some Burning Characteristics of Filter Paper. Combustion Sci. and Tech., vol. 3, no. 3, May 1971, pp. 103-120.
11. Andracchio, Charles R.; and Aydelott, John C.: Comparison of Flame Spreading over Thin Flat Surfaces in Normal Gravity and Weightlessness in an Oxygen Environment. NASA TM X-1992, 1970.
12. Pearce, James P.; Kenzey, Howard J.; and Pippen, David L.: The Effects of Gravity on Flammability. Conference on Materials for Improved Fire Safety. NASA SP-5096, 1970, pp. 137-139.
13. Cochran, Thomas H.; Petrash, Donald A.; Andracchio, Charles R.; and Sotos, Ray G.: Burning of Teflon-Insulated Wires in Supercritical Oxygen at Normal and Zero Gravities. NASA TM X-2174, 1971.
14. Neustein, R. A.; Mader, P. O.; Colombo, G. V.; and Richardson, D. E.: The Effect of Atmosphere Selection and Gravity on Burning Rate and Ignition Temperature. DAC-62431, Advance Biotechnology and Power Dept., McDonnell-Douglas Astronautics Co. (NASA CR-106652), 1968.
15. Stevens, M. R.; Fisher, H. D.; and Breen, B. P.: Investigation of Materials Combustibility, Fire, and Explosion Suppression in a Variety of Atmospheres. AFAPL-TR-68-35, Dynamic Science Corp. (AD-669349), 1968.
16. Schreihans, F. A.: Flammability Characteristics of Some Organic Spacecraft Materials in Zero Gravity. SID-65-640, Space and Information Sys. Div., North American Aviation, Inc. (NASA CR-92833), 1965.
17. Kimzey, J. H.; Downs, W. R.; Eldred, C. H.; and Norris, C. W.: Flammability in Zero-Gravity Environment. NASA TR R-246, 1966.
18. Adelberg, Marvin: Effect of Gravity and Free Stream Velocity Upon Combustion Rate of Space Cabin Materials. TN 176-D-33-11-67, Adelberg Research and Development Lab., Inc., Nov. 1967.
19. Haggard, John B., Jr.; and Cochran, Thomas H.: Hydrogen and Hydrocarbon Diffusion Flames in a Weightless Environment. NASA TN D-7165, 1973.

TABLE I. - FLAME SPREAD RATES FOR CELLULOSE ACETATE SPECIMENS

Specimen thickness, cm	Specimen orientation	Initial chamber conditions		Flame spread rate, cm/sec	
		Pressure, N/cm <sup>2</sup>	Temperature, °C	V <sub>1-g</sub>	V <sub>0-g</sub>
0.0025	Horizontal ↓	3.45	20 ↓	6.7	5.5
.0051		3.45		2.9	2.0
.0122		3.45		1.7	.9
.0025		10.14		7.0	5.5
.0051		10.14		3.2	2.0
.0122		10.14		1.9	1.2
.0025	Vertical	634	-118	10.2	9.7
.0051	Vertical	634	-118	7.8	4.9
.0122	Vertical	634	-118	6.9	3.6

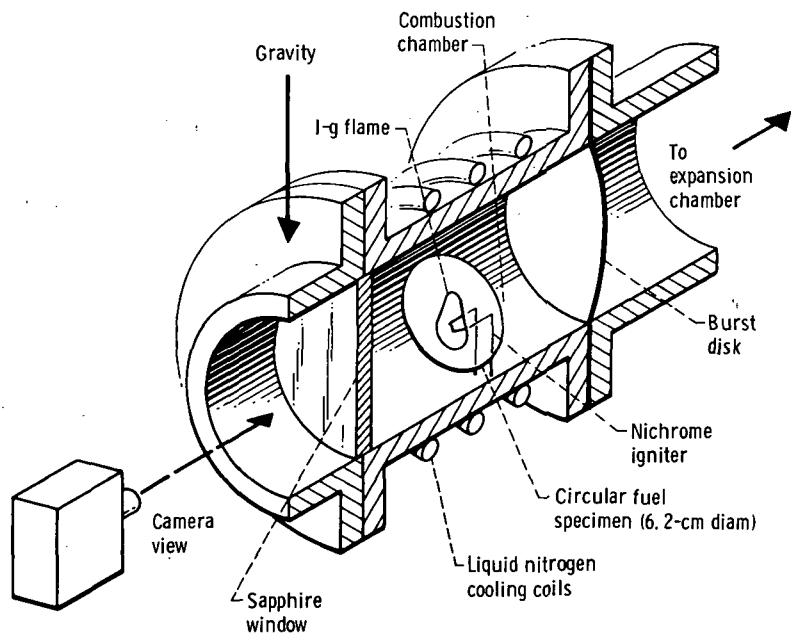


Figure 1. - Schematic diagram of vertically burning fuel specimen used in supercritical oxygen tests.

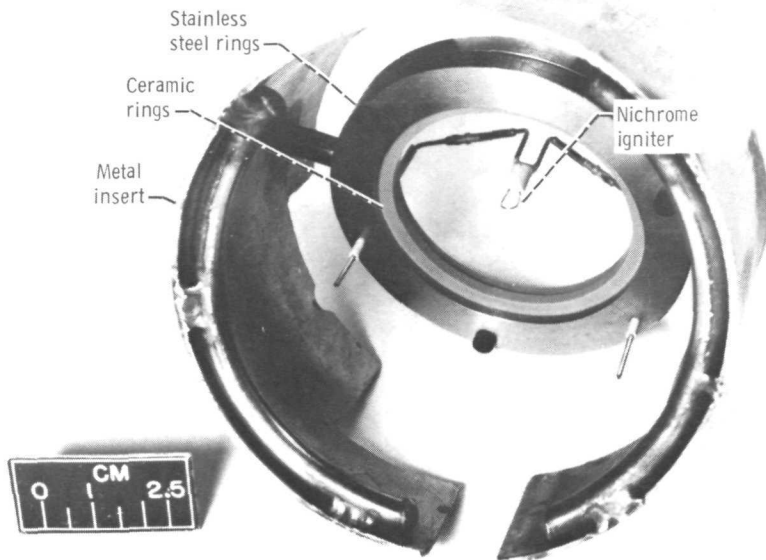


Figure 2. - Specimen holder and ignitor used in supercritical oxygen tests.

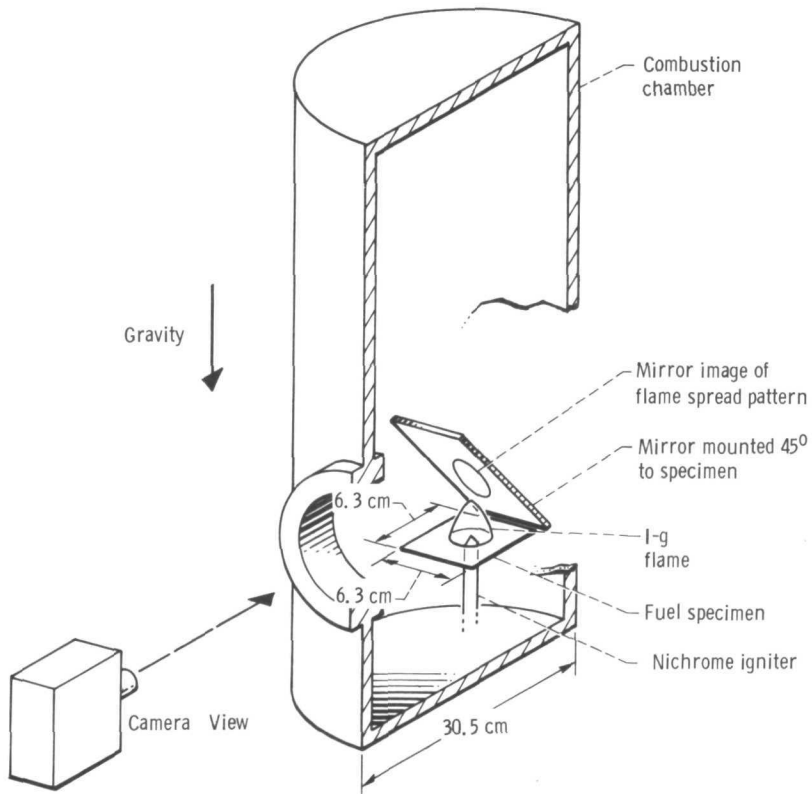


Figure 3. - Schematic of horizontally burning fuel specimen used in low pressure oxygen tests.

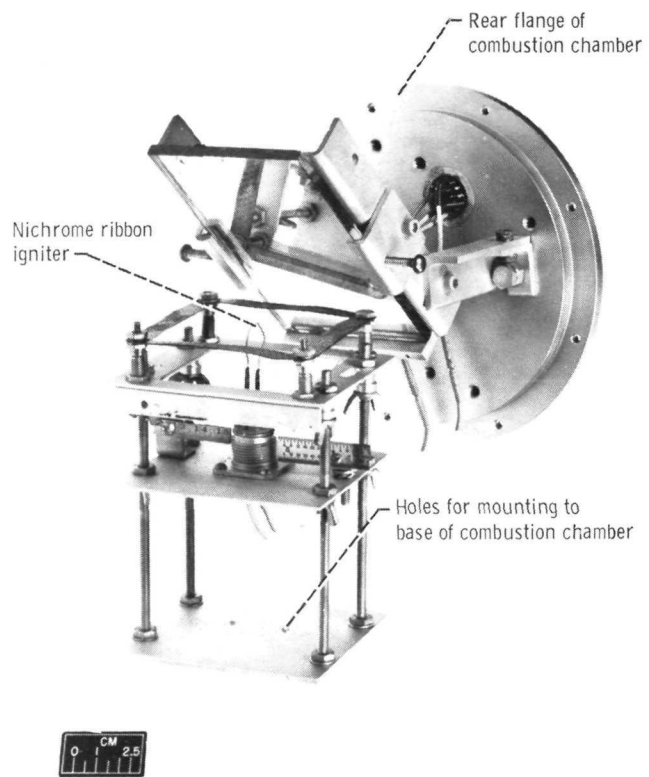
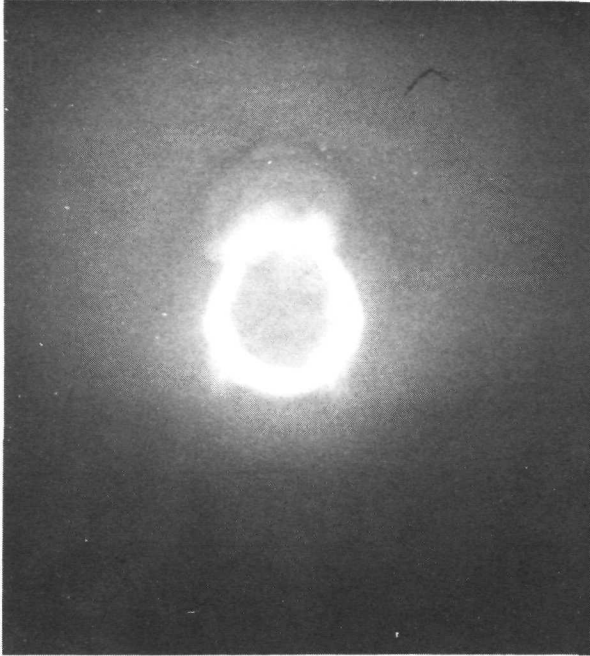
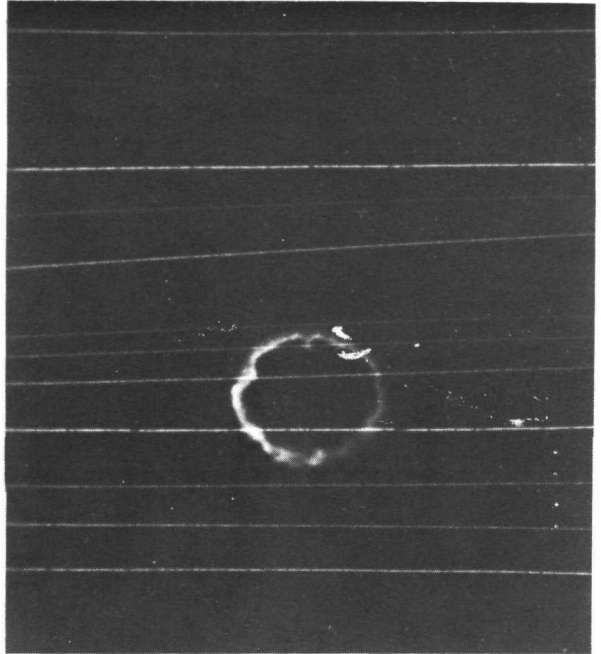


Figure 4. - Specimen holder and igniter used in low pressure oxygen tests.

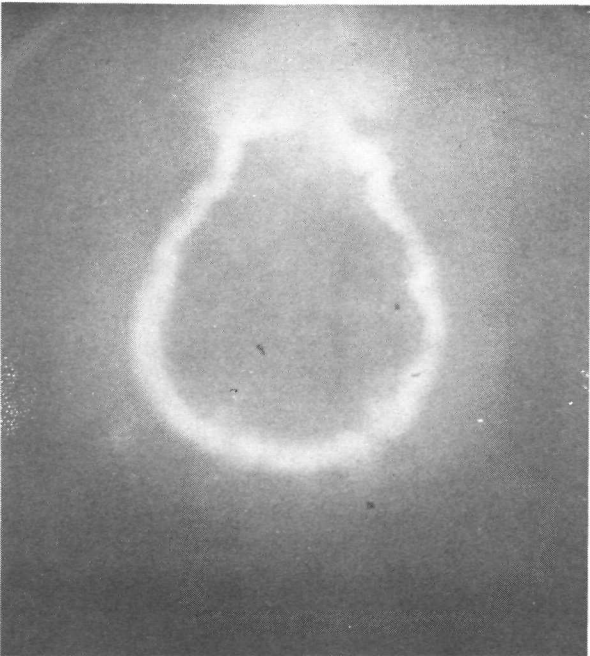




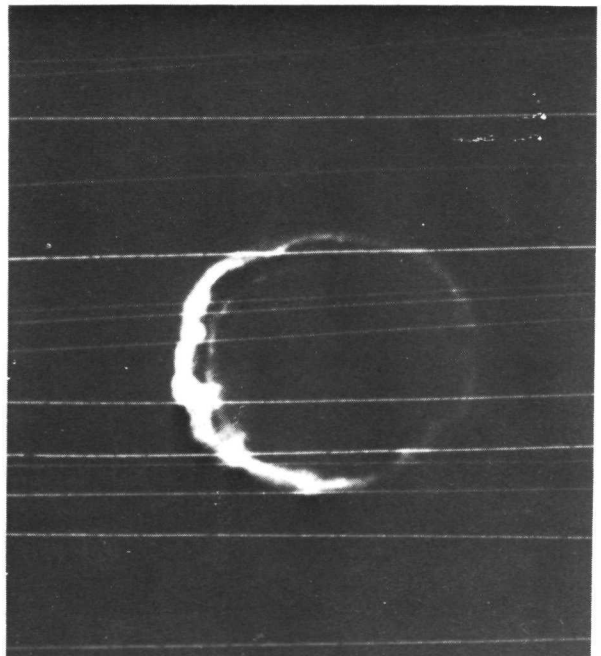
(a) 0.05 Second after ignition; normal gravity.



(b) 0.05 Second after ignition; zero gravity.

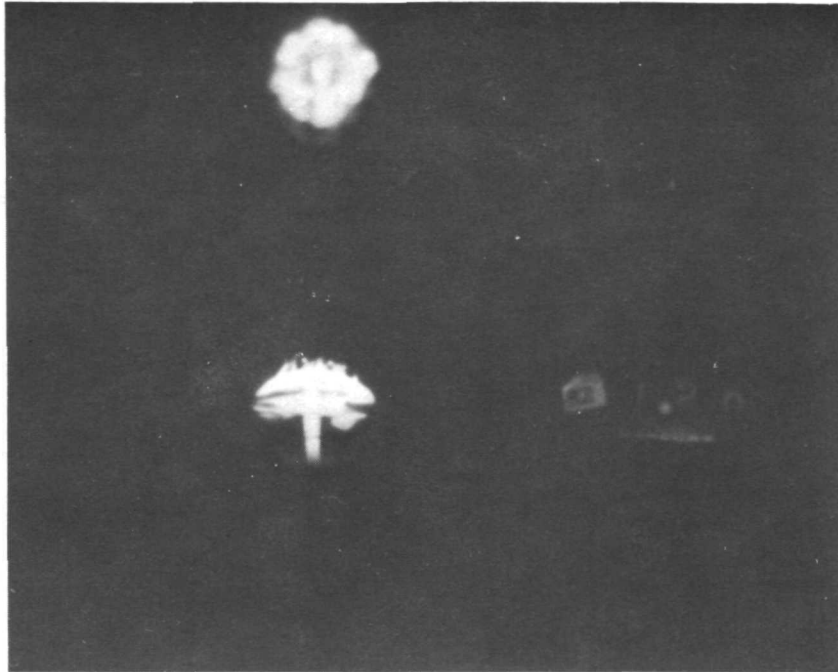


(c) 0.10 Second after ignition; normal gravity.

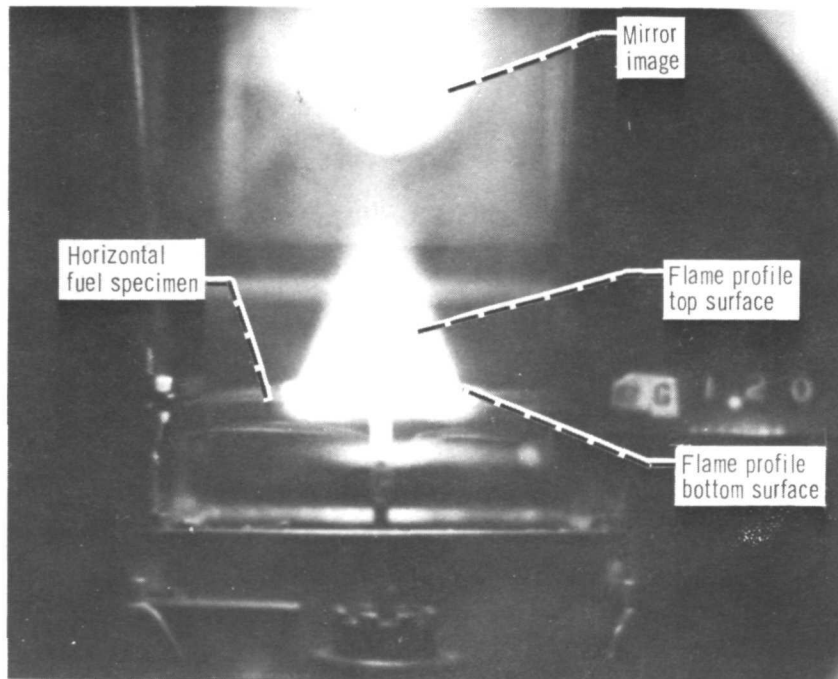


(d) 0.10 Second after ignition; zero gravity.

Figure 5. - Burning of cellulose acetate in supercritical oxygen; normal and zero gravity.

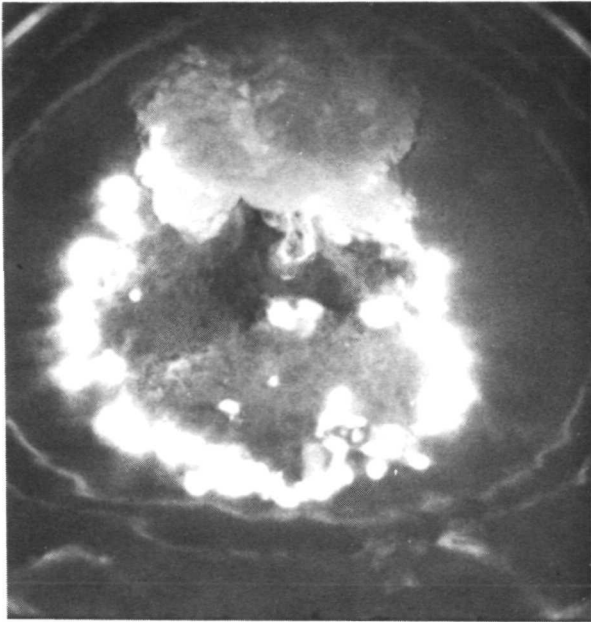


(a) Zero gravity.

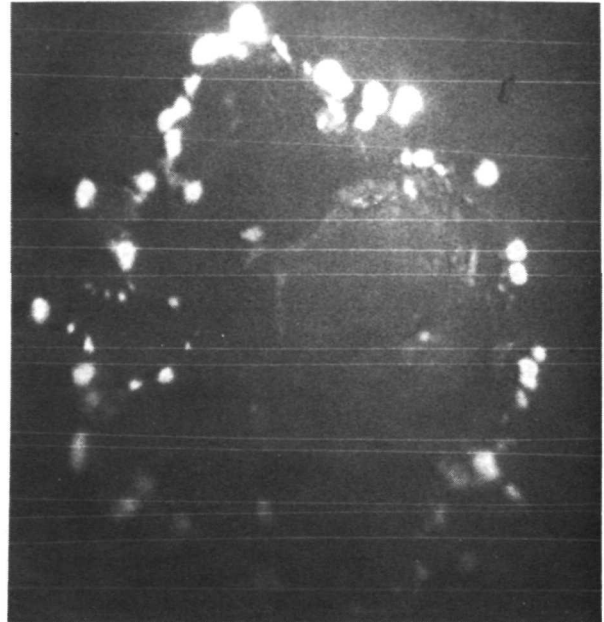


(b) Normal gravity.

Figure 6. - Burning of cellulose acetate in low pressure ( $10.14 \text{ N/cm}^2$ ) oxygen.



(a) Normal gravity.



(b) Zero gravity.

Figure 7. - Burning of stainless steel screen in supercritical oxygen.

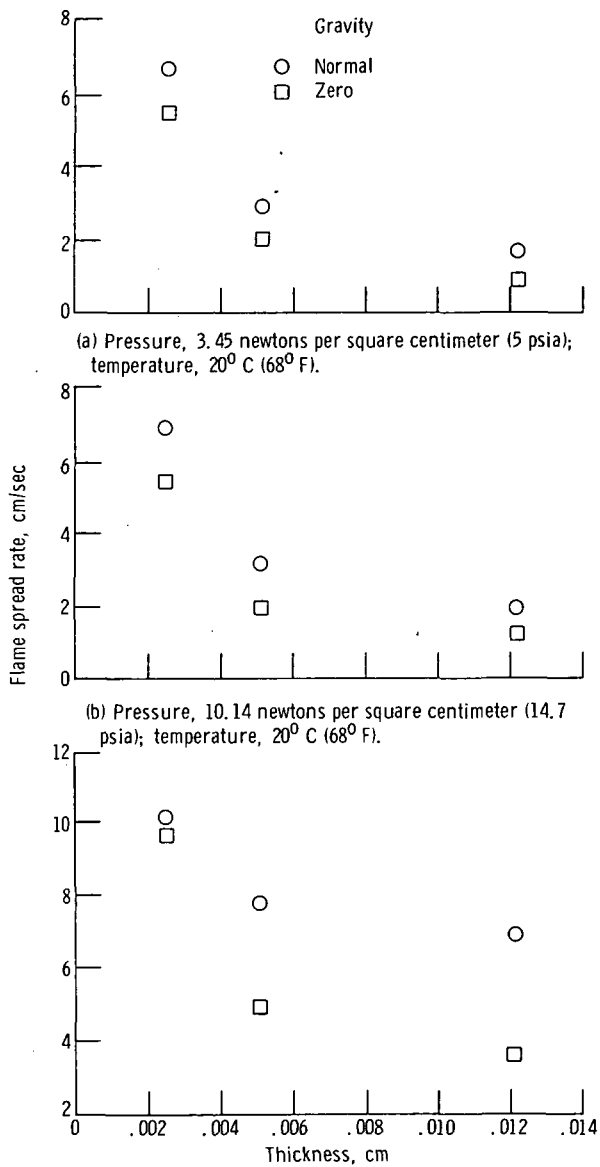


Figure 8. - Effect of thickness on flame spread rate for cellulose acetate specimens.

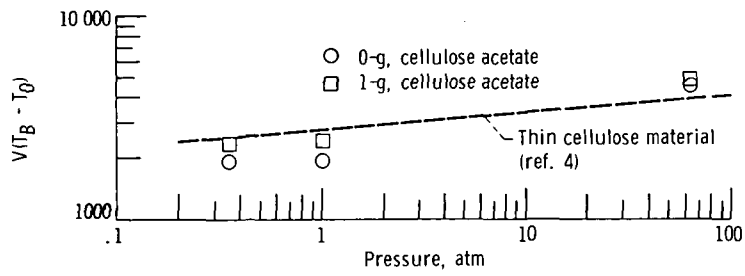


Figure 9. - Thin material behavior with pressure.

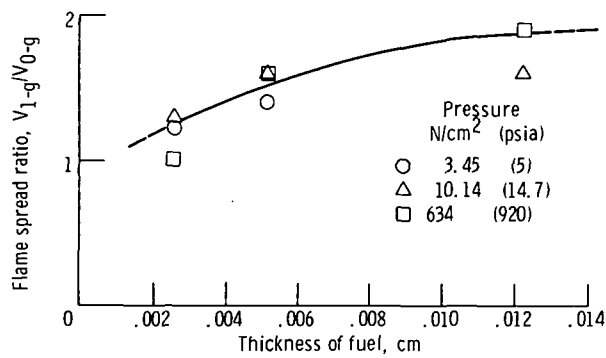


Figure 10. - Comparison of normal and zero gravity flame spread rates with thickness for cellulose acetate specimens.